BIREFRINGENCE OF SPERMATOZOA

II. Form Birefringence of Bull Sperm

IRWIN J. BENDET and JAMES BEARDEN, JR.

From the Department of Biophysics and Microbiology, University of Pittsburgh, Pittsburgh, Pennsylvania 15213. Dr. Bearden's present address is the Department of Pharmacology, Baylor College of Medicine, Houston, Texas 77025.

ABSTRACT

In thermal denaturation experiments on sperm cells, described in the accompanying paper, it was found that squid sperm, when melted, lose both birefringence and morphological shape. Bull sperm, on the other hand, show no change of morphology, but their initial negative birefringence becomes positive. Since this suggested the existence of form birefringence, the influence of solvents of different refractive indices on the observed birefringence was investigated, using a new derivation of the Wiener form birefringence equations which allows direct comparison of Wiener's theory with experimental results. Bull sperm showed form birefringence both before and after melting, while squid sperm showed none. Quantitative application of the general form of the Wiener equations to these results gave values for the refractive index and intrinsic birefringence of bull sperm cells. Application of the specific forms of the Wiener equations showed that neither of these descriptions of idealized systems was adequate to describe completely the form birefringence of bull sperm, but that the equation for platelike submicroscopic structures was more nearly an accurate fit to the data than that for rodlike structures.

INTRODUCTION

It was mentioned in the accompanying paper on birefringence melting of sperm cells that the initial negative retardation of the bull sperm, when melted, did not simply go to zero, but became positive. Since the same positive value was reached at the end of each melting experiment in ethylene glycol, it was assumed that it reflected some definite physical characteristic of the cell. This behavior would suggest the existence of a weak positive form birefringence which remained unchanged after melting, in addition to a stronger negative intrinsic birefringence (lost during melting), for the bull sperm cell, but not for the squid sperm. The experiments described in this paper were performed to test this hypothesis.

The phenomenon of form birefringence was first explained by Wiener (1912), who showed that certain types of submicroscopic structures would appear birefringent because of their form and the difference between their refractive index and that of the solvent, rather than because of the intrinsic birefringence of their chemical structure. He proposed two equations to describe the form birefringence of two types of idealized systems. The first system was a set of parallel cylindrical rods, impermeable to the solvent, whose diameter (each rod) was small compared to the wavelength of light. The optic axis of such a system, which is defined as the direction along which no birefringence is observed (Hartshorne and Stuart,

1970), would be parallel to the rods, and the form birefringence of such a system with respect to this axis is described by the following equation:

$$n_e^2 - n_o^2 = \left[\frac{V_1V_2(n_1^2 - n_2^2)^2}{V_2n_1^2 + (1 + V_1)n_2^2}\right], \qquad (1)$$

where $(n_e - n_o)_f$ is the form birefringence of the system (note that the left side of the equation is slightly different from this); V_1, the volume fraction occupied by the solid phase (the rods); V_2, the volume fraction of the liquid phase ($V_1 + V_2 \equiv 1$); n_1, the refractive index of the rods; and n_2, the refractive index of the solvent.

The second type of system considered by Wiener was a set of stacked plates, also impermeable to the solvent, whose thickness (each plate) was small compared to the wavelength of light. The optic axis of this system would be perpendicular to the plates, and the form birefringence with respect to this axis would be described by:

$$n_e^2 - n_o^2 = -\left[\frac{V_1V_2(n_1^2 - n_2^2)^2}{V_2n_1^2 + V_1n_2^2}\right], \qquad (2)$$

where all the symbols have the same meaning as before. The negative sign in the second equation, which is for measurements referred to the optic axis, will be positive in the forms of this equation used here, since the reference axis used is parallel, rather than perpendicular, to the plates.

These equations have one obvious feature: for $n_1 = n_2$, the form birefringence is zero, and total birefringence will be a maximum or minimum. This feature has been used a number of times to detect the existence of form birefringence in the type of experiment described by Ambronn (1916) and Ambronn and Frey (1926). Generally, the procedure is to use solvents of different refractive indices, and to plot the total birefringence of the system as a function of n_2. If this produces a curve which is roughly parabolic (an Ambronn curve), then the system has form birefringence, and the maximum or minimum of the curve can be used to determine n_1, the refractive index of the object in question, and $(n_e - n_o)_i$, the intrinsic birefringence, if any. For example, this procedure has been used by Frey (1926) on incinerated barley awns, Lauffer (1938) on tobacco mosaic virus, Frey-Wyssling and his associates (1948, 1964, 1965) on plant cell walls and chloroplasts, and Sato et al. (1971) on isolated mitotic spindles, to show that all these systems had form birefringence. It was also used by Schmidt (1928) on cuttlefish sperm, to show that they had no form birefringence.

None of these previous experimenters with the exception of Sato et al. (1971), however, attempted to apply the quantitative details of the Wiener equations to their experimental results. One reason for this, as pointed out by Frey-Wyssling (1948), is that no biological object of any interest is known to possess the exact characteristics of Wiener's ideal systems. The systems rarely consist of perfect rods or plates, and are almost always permeable to the solvent, a fact which can also affect the optical properties (Hartshorne and Stuart, 1970, p. 565). A second reason is that the Wiener equations are not written in terms of quantities which are directly measured experimentally; this is related to the first reason since, in the absence of known ideal systems, few attempts have been made to compare experiment and theory in detail. Derivations have been presented for systems in which V_1 was very small (Peterlin and Stuart, 1939; Cassim et al., 1968), but none of these are applicable to very concentrated systems, such as the inside of a sperm cell. Nor is the procedure used by Sato et al. (1971) useful for this system, since it requires independent knowledge of important parameters of the system.

This paper approaches the problems mentioned above by deriving forms of the original Wiener equations which are directly applicable to experimental results from systems having large solid volume fractions. The general form of these equations may be used for any system displaying form birefringence, even those with none of the ideal characteristics described above, since its application requires no assumptions concerning the exact shape, orientation, or impermeability of the submicroscopic elements. In order to apply the more specific forms of these equations, such assumptions are required, but their validity may be directly tested for the particular experimental system. The methods described here, therefore, should be useful for a variety of systems besides the sperm cells studied in this paper.

MATERIALS AND METHODS

The derivation of the Wiener equations, written in terms of the experimentally determined quantities, is contained in the Appendix at the end of this paper. As stated there, it was not possible to derive an exact relationship between the measured birefringence, $(n_e - n_o)$, and the refractive index of the solvent, n_2,

but close approximations could be derived for this experimental situation, involving cubic or higher order equations, all in terms of powers of $(n_2)^2$.

Experimental data on the influence of the refractive index of the solvent on the measured birefringence of the cells were obtained for bull sperm, both before and after melting, and squid sperm, before melting. Since, as shown in the paper on birefringence melting, squid sperm lose their morphological form as well as their birefringence when heated, no experiments were done on melted squid sperm. Also, because of the extremely small retardations associated with human spermatozoa, no experiments were done on these samples either. Several different solvent systems were investigated, but it was found that most nonpolar organic solvents, such as the quinoline-dioxane mixtures used by Inoué and Sato (1966), had deleterious effects on the cell morphology. The solvents finally used were mixtures of ethylene glycol (n_D = 1.4375), aniline (n_D = 1.5863), and *m*-bromoaniline (n_D = 1.6260), since these liquids were miscible, had no visible adverse effect on the cells, and covered a range of refractive indices which included that of the cells.

For each experiment, 14–16 sperm samples in ethylene glycol were pelleted in centrifuge tubes at 5000 *g* for 10 min. After the pellets were drained as much as possible, they were resuspended in mixtures of the three solvents, with the amount of each adjusted so that a range of refractive indices from about 1.45 to 1.60 would be covered in 0.01 increments from one tube to the next. Since some of the original solvent was retained in the pellet and in the cells, it was necessary to wait until after complete equilibration had occurred (at least 1 wk), and measurements of the birefringence had been made, to determine the exact refractive index of the solvent in each tube. This was done by sedimenting the cells at 12,000 *g* (10,000 rpm) for 10 min to form a hard pellet. Then the refractive index of the supernatant fluid in each tube was measured on a Zeiss Abbé Refractometer (accurate to ± 0.0002).

For statistical purposes, the retardations of 50 cells from each tube were measured using the Brace-Köhler compensator (the use of which is described in the accompanying paper), with the "A" axis of each cell (both species) oriented at 45° to the crossed polaroids of the microscope (see Fig. 1 in the accompanying paper for the reference axes used for each species). Bull sperm were measured with their "B" axes parallel to the microscope axis (oriented "on edge"). In addition, for the unmelted bull sperm samples, the retardations of 10 cells from each sample were measured whose "C" axes were parallel to the optic axis of the microscope ("flat" oriented); these cells were oriented by rotating the microscope stage until maximum birefringence was observed, since this was not always when the "A" axis was at 45° to the crossed polaroids.

The average birefringence, standard error of the mean, and 95% confidence limits (from Student's distribution, Walker and Lev, 1958, p. 271) were calculated for each sample. Least-squares fits were calculated for the coefficients of the cubic-equation approximation, using standard programs 13.20 and 15.03 for the Olivetti-Underwood "Programma 101" calculator. These fitted coefficients were used to draw Ambronn curves (birefringence vs. refractive index of the solvent) and, as described in the Appendix, to calculate the refractive index of the cell, n_1, and the intrinsic birefringence, $(n_e - n_o)_i$, using the general form of the equation. The possibility that one of the exact forms of the Wiener equation would describe the form birefringence of the sperm nucleus was tested by using both exact forms to calculate the volume fractions, V_1 and V_2.

RESULTS

Quantitative data on the influence of the refractive index of the solvent on the measured birefringence of the various samples are presented in Table I. It can be seen from these results that bull sperm, when their retardations are measured along the "B" axis, show a considerable amount of form birefringence both before and after melting. A least-squares fit to these data points, using the cubic approximation described in the Appendix, produced the Ambronn curves shown in Figs. 1 and 2.

For the bull sperm before melting (Fig. 1), the cubic equation best fitting the points is

$$\begin{aligned} y &= (n_e - n_o) \times 10^3 \\ &= (11.680473)x^3 - (51.225649)x^2 \\ &\quad + (50.415246)x + (8.703123), \end{aligned} \tag{3}$$

where $x \equiv (n_2)^2$, as described in the Appendix. Setting the first derivative of this equation equal to zero gives the minimum, from which it can be determined that

$$n_1 = 1.5158.$$

At this point $y = -4.209$, and the intrinsic birefringence of the cell is

$$(n_e - n_o)_i = -0.00421.$$

For the bull sperm after melting, the best fitted

TABLE I A

Results of Form Birefringence Experiments Bull Sperm, Unmelted*

(n_2)	($n_e - n_o$) × 10^3 (Measured along "B" axis)	($n_e - n_o$) × 10^3 (Measured along "C" axis)‡
1.4522	−3.256 ± 0.049	−2.01 ± 0.34
1.4607	−3.486 ± 0.055	−2.18 ± 0.36
1.4691	−3.672 ± 0.055	−1.94 ± 0.32
1.4712	−3.764 ± 0.064	−2.39 ± 0.49
1.4858	−3.907 ± 0.059	−2.13 ± 0.30
1.4934	−4.037 ± 0.059	−2.54 ± 0.41
1.5034	−4.091 ± 0.053	−2.07 ± 0.30
1.5104	−4.235 ± 0.044	−2.26 ± 0.30
1.5168	−4.266 ± 0.045	−2.35 ± 0.43
1.5295	−4.246 ± 0.048	−2.33 ± 0.47
1.5396	−4.024 ± 0.038	−2.43 ± 0.51
1.5499	−3.928 ± 0.049	−2.01 ± 0.34
1.5530	−3.745 ± 0.047	−2.33 ± 0.53
1.5640	−3.553 ± 0.046	−2.31 ± 0.51
1.5659	−3.436 ± 0.051	−2.07 ± 0.36
1.5703	−3.314 ± 0.052	−2.31 ± 0.45

* Figures after the "±" signs in the birefringence columns for all sample groups in this table are 95% confidence limits (from Student's distribution for the appropriate sample size). Thicknesses used in calculating birefringence were from Altman and Dittmer (1962).

‡ In calculating the values in this column, it was assumed that $C = 0.3$ μm, in order to find maximum values for the birefringence in this direction, since this is the lowest of the different values given by Altman and Dittmer (1962) and Benedict (1964).

TABLE I B

Results of Form Birefringence Experiments Bull Sperm, Melted

(n_2)	($n_e - n_o$) × 10^3 (Measured along "B" axis)
1.4625	1.500 ± 0.067
1.4805	1.390 ± 0.047
1.4874	1.195 ± 0.055
1.4939	0.947 ± 0.042
1.5060	0.840 ± 0.47
1.5149	0.595 ± 0.042
1.5212	0.402 ± 0.022
1.5313	0.230 ± 0.015
1.5463	0.097 ± 0.010
1.5608	(*)
1.5687	(*)
1.5744	0.070 ± 0.010
1.5802	0.137 ± 0.010
1.5877	0.225 ± 0.022

* Retardations for these two samples were below the limits of measurement for this microscope, so no quantitative values were obtained. Qualitatively, their retardations appeared to be either zero or positive and less than half those of the samples above and below them in the table, so a value of 0 + 0.020 was used for calculating the coefficients of Equation (4) and drawing Fig. 2.

Ambronn curve (Fig. 2) is described by

$$y = (n_e - n_o) \times 10^3 = (4.495346)x^3 - (14.561774)x^2 - (9.737188)x + (45.227653). \quad (4)$$

From this equation and its first derivative, the following values were obtained:

$$n_1 = 1.5665$$

$$(n_e - n_o)_i = 0.00007$$

Considering the error limits shown in Fig. 2, this value for intrinsic birefringence is probably not significantly different from zero.

Application of the specific form of the Wiener equation for rodlike structures to the data in Figs. 1 and 2 resulted in values for V_1 and V_2 which were imaginary. Such values, which can occur when the value of F in the equation for rods exceeds ($\frac{1}{16}n_1^3$), are a definite indication that the submicroscopic structures responsible for the form birefringence in both melted and unmelted bull sperm are not well approximated by Wiener's ideal system of rods. The specific Wiener equation for platelike structures came much closer to describing the data obtained, since the following values, calculated from it, are all real and lie within reasonable limits:

For bull sperm before melting, $\begin{cases} V_1 = 0.72 \\ V_2 = 0.28 \end{cases}$;

For bull sperm after melting, $\begin{cases} V_1 = 0.83 \\ V_2 = 0.17. \end{cases}$

There are some indications here also, however, that the Wiener equation, derived for an idealized system of plates, does not adequately describe the form birefringence of the bull sperm nuclei. As shown in the Appendix, a cubic equation should fit the points generated by the Wiener equations very closely, yet the closest possible cubic fits to the actual data in Figs. 1 and 2 lie outside the 95% confidence limits of a number of experimental points. Secondly, although the Wiener equations predict that F will decrease in value with increasing n_2, the experimental values of F actually increase in both figures. Such observations raise serious doubts about the accuracy of the volume fractions calculated above, and indicate that, while

TABLE I C

Results of Form Birefringence Experiments
Squid Sperm, Unmelted

(n_2)	Compensator angle*
1.4460	23.18° ± 0.10°
1.4649	23.25° ± 0.13°
1.4685	23.23° ± 0.12°
1.4797	23.31° ± 0.12°
1.4881	23.27° ± 0.11°
1.4932	23.26° ± 0.13°
1.5101	23.05° ± 0.12°
1.5168	23.09° ± 0.13°
1.5260	23.31° ± 0.13°
1.5352	23.05° ± 0.13°
1.5512	23.15° ± 0.13°
1.5640	23.22° ± 0.15°
1.5752	23.21° ± 0.13°
1.5817	23.11° ± 0.15°
1.5868	23.20° ± 0.14°
1.5947	23.09° ± 0.14°

* The value of the compensator angle for each sample shown in this column would normally be subtracted from 43.3°, the zero point of this compensator, to give θ, the angle used to find the birefringence. Since the angles obtained here showed no indication of form birefringence, or any significant difference from each other, they were all averaged together to give a compensator angle of 23.19°, which was then used to calculate the results for retardation and birefringence.

these results rule out the existence of an ideal system of rods, they do not prove the existence of any other system of submicroscopic elements.

It may be seen in Table I (A and C) that neither the measurements on unmelted bull sperm, measured along their "C" axes instead of the "B" axes as above, nor those on squid sperm, revealed any dependence of birefringence on the refractive index of the solvent. For the former, the retardations measured were extremely small and the associated errors in birefringence are correspondingly large, due to the small "C" dimension. Consequently, the possibility that there may be some form birefringence effect on the measurements taken along the "C" axis cannot be ruled out, but no such effect is evident. This would mean that for the form birefringence, the optic axis is the "C", rather than the "A", axis (from the definition given earlier for the optic axis); and all of the form birefringence values measured along the "B" axis would be negative with respect to the "C"

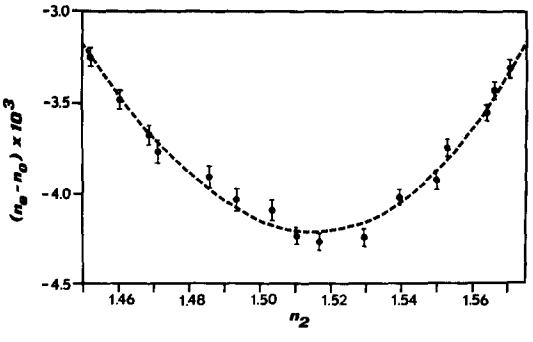

FIGURE 1 Ambronn curve showing form birefringence of unmelted bull sperm in mixtures of ethylene glycol, aniline, and *m*-bromoaniline. Error bars shown represent 95% confidence limits for each experimental point. The heavy dashed line represents values of Equation (3).

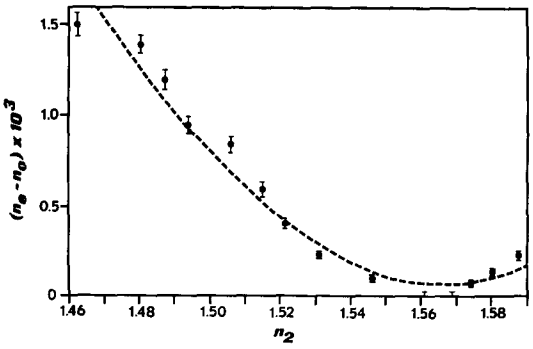

FIGURE 2 Ambronn curve for melted bull sperm. Same solvent mixtures and error limits as in Fig. 1; dashed line represents values of Equation (4). All values for experimental points from Table I, for both figures; see this table for an explanation of the two points for which only error bars are shown above.

(optic) axis, as predicted in Equation (2) in the Introduction.

Cells which were oriented so that their "A" axes were parallel to the direction of observation in the microscope ("head-on" orientations) were seen rarely, so no series of quantitative measurements were made on them. Occasional qualitative observations on such cells in the unmelted preparations, however, showed that they had varying amounts of positive or negative birefringence, depending on their orientation, with respect to the "B" axis; in the melted preparations, such cells always showed positive retardations with respect to the "B" axis. This behavior would not be expected if the structures responsible for form birefringence were rodlike, an observation also noted

by Koehler (1970), since for such structures the "A" axis would constitute the optic axis.

The data in Table I A for measurements along the "C" axis also show that, even after correcting for the much smaller thickness in this direction, the birefringences measured are significantly smaller in magnitude than those measured along the "B" axis. The absence of cylindrical symmetry in the bull sperm head, therefore, may reflect more fundamental asymmetries in the submicroscopic structures of the nucleus.

It was mentioned earlier that the measurements on squid sperm also showed no dependence of birefringence on refractive index of the solvent, as shown in Table I C. The error in these measurements is much smaller than that for the bull sperm measured along the "C" axis, so that the existence of any significant amount of form birefringence in squid sperm seems to be ruled out by these figures. This agrees with the observation of Schmidt (1928) on sperm nuclei of the cuttlefish, a closely related species.

Since no significant differences seemed to exist among the squid sperm samples as a function of refractive index, all of the measurements were averaged together to obtain a more accurate value for the intrinsic birefringence. The average retardation (with 95% confidence limits), when calculated by the exact formula for the Brace-Köhler compensator (given in the accompanying paper), is

$$R = -35.63 \pm 0.18 \text{ nm.}$$

Use of the approximate formula ($R = R_0 \cdot \sin 2\theta$) resulted in an average value of

$$R = -36.42 \pm 0.20 \text{ nm.}$$

This is also an indication of the maximum error (about 2%) caused by use of the approximate formula in other parts of this work. The retardation, calculated by the exact formula, and a cell thickness of 1.4 μm for *Loligo pealii* (Sato and Inoué, 1964), means that the average cell birefringence is

$$(n_e - n_o) = -0.0254 \pm 0.0001.$$

This is in agreement with the value of -0.02 reported previously for the same species (Sato and Inoué, 1964; Inoué and Sato, 1966).

DISCUSSION

The results of this paper indicate that there are no submicroscopic structures in squid sperm nuclei which show form birefringence, but that such structures do exist in bull sperm. This organization of molecules within the bull sperm head into larger elements, having a semicrystalline structure different from that of the structures responsible for the intrinsic birefringence, represents an additional way in which the bull and squid sperm differ. This does not seem to be related to the presence of disulfide bonds in the bull sperm, since the results of the accompanying paper show that bull sperm in β-mercaptoethanol have retardations before and after melting which are almost equal to those of cells without β-mercaptoethanol, implying that similar amounts of form birefringence are present in each case.

The present results are interesting when compared to those of Koehler (1966, 1968, 1970), who has shown that submicroscopic nucleoprotein structures can be seen in freeze-etched bull and rabbit sperm. His proposal that these structures are platelike would be consistent with the qualitative observations of this paper on the birefringence along different axes, and with the fact that the Wiener equation (specific form) for platelike structures more closely approximates these data. The existence of platelike structures has been questioned by Lung (1968), who observed fibrillar structures in bull sperm; but he also mentioned that his treatment could have separated the plates, if originally present, into a finer substructure. Observation of freeze-etched bull sperm cells after some of the treatments used in these papers might yield useful information concerning the correlation of optical and ultrastructural properties of the sperm nucleus; such a correlation, as noted by Koehler (1970), could help to reveal the actual structure of mammalian sperm nucleoprotein.

This discussion has assumed that the same nucleoprotein structures observed by Koehler (1966, 1968) and Lung (1968) are responsible for the form birefringence of bull sperm. Because of the limited resolution of the light microscope, however, it is also possible that some other elements, such as the membrane structures shown by Koehler (1966) or the external lipoprotein complex reported by Dallam and Thomas (1953), could cause the form birefringence; or that it represents a sum of birefringences of nucleoprotein and other structures. Resolution of this question would be necessary before these, or any other, birefringence data could be used to their full potential in determining the structure of the sperm nucleus.

We wish again to thank Dr. Charles Kiddy and Dr. Shinya Inoué for their help in providing essential materials and methods. The discussions with Dr. Max A. Lauffer and Dr. Charles L. Stevens, and the equations derived by Dr. Lauffer, which led to the theoretical treatment of the form birefringence presented in the Appendix, are also gratefully acknowledged.

Preliminary results were presented at the annual meeting of the Biophysical Society, February 15-18, 1971.

This work was supported by grants 5 F01 GM 41796-03 and GM 10403 from the National Institutes of Health, United States Public Health Service.

This is publication No. 182 of the Department of Biophysics and Microbiology of the University of Pittsburgh.

Received for publication 11 August 1971, and in revised form 21 June 1972.

APPENDIX

Derivation of Theoretical Equations for Form Birefringence

The equations proposed by Wiener to describe the form birefringence of two types of ideal systems were presented in the Introduction to this paper. In order to relate these equations to experimentally determined values, it is first necessary to rewrite them in terms of the birefringence which is actually measured in the experiments. The left side of either equation can be factored into two terms, thus:

$$(n_e^2 - n_o^2) = (n_e - n_o)_f\,(n_e + n_o) = (n_e - n_o)_f \left[2\left(\frac{n_e + n_o}{2}\right)\right], \quad (5)$$

where $(n_e - n_o)_f$ is the form birefringence, and $\left(\frac{n_e + n_o}{2}\right)$ is the average refractive index of the system, n_m. An equation for n_m is also given by Wiener (1912) and Lauffer (1938):

$$n_m^2 = \left[\frac{(1 + V_1)n_1^2 + (1 - V_1)n_2^2}{(1 - V_1)n_1^2 + (1 + V_1)n_2^2}\right](n_2)^2, \quad (6)$$

where all symbols have the same meaning as before.

For application to general experimental results, in which the cells can have both intrinsic birefringence, $(n_e - n_o)_i$, assumed to be constant, and form birefringence, it is also necessary to rewrite the left side in terms of the total measured birefringence, $(n_e - n_o)$:

$$(n_e - n_o) = (n_e - n_o)_f + (n_e - n_o)_i. \quad (7)$$

The specific form of the Wiener equation for a system of rods, then is

$$(n_e - n_o) = \left\{\frac{V_1V_2}{[V_2n_1^2 + (1 + V_1)n_2^2](2n_2)} \cdot \sqrt{\frac{(1 + V_1)n_1^2 + (1 - V_1)n_2^2}{(1 - V_1)n_1^2 + (1 + V_1)n_2^2}}\right\} X(n_1^2 - n_2^2)^2 + (n_e - n_o)_i \quad (8)$$

and the specific form for a system of plates is

$$(n_e - n_o) = \left\{\frac{V_1V_2}{[V_2n_1^2 + V_1n_2^2](2n_2)} \sqrt{\frac{(1 + V_1)n_1^2 + (1 - V_1)n_2^2}{(1 - V_1)n_1^2 + (1 + V_1)n_2^2}}\right\} X(n_1^2 - n_2^2)^2 + (n_e - n_o)_i. \quad (9)$$

The entire term in each equation inside the braces, { }, may be defined as F, the Wiener form factor, with the understanding that the value of F for platelike structures differs from the value for rodlike structures. A general form of either equation, then, can be written more simply by replacing the large term in braces with F, and by defining $x \equiv (n_2)^2$:

$$(n_e - n_o) = Fx^2 - (2n_1^2F)x + [F(n_1)^4 + (n_e - n_o)_i] \quad (10)$$

If F were a constant, this would be a simple quadratic equation in terms of x and $(n_e - n_o)$, both of which are experimentally measurable. Unfortunately, F is not constant, since it contains n_2, (see Equations [8] and [9]) and it has not been possible to derive any form of the equation in which a corresponding term is a constant. It has been necessary, therefore, to determine to what extent F can be approximated in this experimental system by simpler terms.

In order to do this, a set of possible theoretical values was generated for each type of system (plates and rods) for F, using reasonable values for the terms it contains. The values of $V_1 = 0.42$ and $V_2 = 0.58$ for bull sperm were taken from Benedict (1964, p. 121); since these represent volume fractions for the entire cells, the value of V_1 in the nucleus is probably higher than this, but it was also determined by separate calculations that

values of V_1 between 0.30 and 0.70 do not greatly affect the values of F. It was assumed that $n_1 = 1.5700$ (an approximate value determined by preliminary experiments) and $(n_e - n_o)_i = 0$, for simplicity. The resulting values of F, over an interval of solvent refractive indices from 1.30 to 1.70, are shown in Table II and graphed as a function of $[(n_2)^2]$ in Fig. 3.

From these calculated values, it can be seen that the representation of F by a constant is not a very good approximation for this system. A much more accurate approximation of the values of F shown in Fig. 3 would be a straight line, of the form

$$F = Mx + B, \tag{11}$$

where M is the slope and B the y-intercept of a line through the points. It was also shown, in an algebraic analysis of this problem by Dr. Max Lauffer, that the approximation of F by a straight line does not depend on the particular values used to derive the figures in Table II, but only upon the condition that n_2 differs from n_1 by less than 10%. This approximation, put into Equation (10) for F, would give the following expansion of that equation:

$$\begin{aligned}(n_e - n_o) &= [Mx + B]x^2 - 2n_1^2[Mx + B]x \\ &\quad + [Mx + B]n_1^4 + (n_e - n_o)_i \\ &= Mx^3 + (B - 2n_1^2M)x^2 \\ &\quad + (n_1^4M - 2n_1^2B)x + Bn_1^4 \\ &\quad + (n_e - n_o)_i\end{aligned} \tag{12}$$

This can be represented as a cubic equation,

$$\begin{aligned}y \equiv (n_e - n_o) \times 10^3 \\ = a_3x^3 + a_2x^2 + a_1x + a_0,\end{aligned} \tag{13}$$

the coefficients of which may be determined by the best fit to the experimental points. For any system which follows the Wiener equations, the cubic equation represents the degree of complexity which is both necessary and sufficient to fit experimental data. This treatment is not limited to such ideal systems, however, since Equation (13) represents only the first four terms of the general formulation of a power series,

$$\begin{aligned}y = a_0 + a_1x + a_2x^2 + \cdots + a_nx^n \\ = \sum_{i=0}^{n} [a_ix^i].\end{aligned} \tag{14}$$

By the inclusion of a sufficient number of terms in the series, the Ambronn curve for any system in which the birefringence varies as a smooth function of the refractive index of the solvent may be approximated to any desired degree of accuracy. The requirement that birefringence be a "smooth" function of n_2 includes the assumptions that y, $\left(\frac{dy}{dx}\right)$, and $\left(\frac{d^2y}{dx^2}\right)$ exist and are continuous at each value of n_2, and that $\left(\frac{dy}{dx}\right)$ is monotonically in-

TABLE II

Theoretically-Calculated Values of Wiener Form Factor, F

n_2	$(n_2)^2$	F (plates)	F (rods)
1.30	1.6900	0.040486	0.022619
1.32	1.7424	0.039714	0.021988
1.34	1.7956	0.038961	0.021380
1.36	1.8496	0.038226	0.020794
1.38	1.9044	0.037509	0.020229
1.40	1.9600	0.036809	0.019683
1.42	2.0164	0.036125	0.019157
1.44	2.0732	0.035457	0.018648
1.46	2.1316	0.034806	0.018157
1.48	2.1904	0.034168	0.017683
1.50	2.2500	0.033546	0.017225
1.52	2.3104	0.032937	0.016781
1.54	2.3716	0.032341	0.016353
1.56	2.4336	0.031759	0.015938
1.58	2.4964	0.031190	0.015537
1.60	2.5600	0.030633	0.015149
1.62	2.6244	0.030088	0.014774
1.64	2.6896	0.029555	0.014410
1.66	2.7556	0.029033	0.014058
1.68	2.8224	0.028522	0.013717
1.70	2.8900	0.028022	0.013387

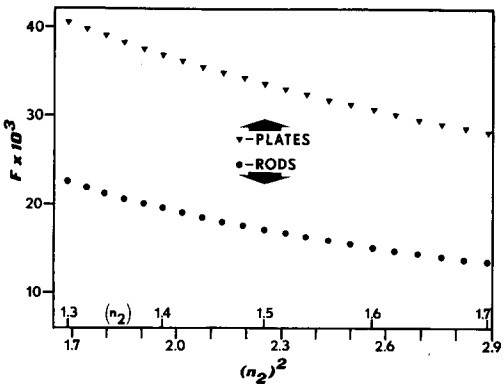

FIGURE 3 Theoretical values of F, the Wiener form factor, as a function of n_2^2. Values shown for platelike and rodlike structures are taken from Table II.

creasing or decreasing over the interval of n_2, but includes no assumptions concerning the shape, orientation, impermeability, or other ideal behavior of the submicroscopic elements responsible for the form birefringence. Equation (14) can be used to describe the birefringence not only for a system of impermeable, perfectly oriented elements of unknown shape (and therefore unknown value of F, the form factor) but also for such examples of nonideal systems as (*a*) elements of differing size and shape, and/or imperfect orientation; (*b*) elements which are reduced in size by one of the solvents used, so that V_1 and V_2 are also variable; (*c*) elements which adsorb one of the solvents so that it takes on a semicrystalline orientation, a possibility mentioned by Hartshorne and Stuart (1970, p. 565) which may be significant in this paper, since crystals of aniline are birefringent. Since none of these systems would be accurately described by either specific form of the Wiener equations, calculation of the volume fractions from birefringence data would be impossible, but good fitting of Equation (14) to birefringence data of such systems would allow more accurate calculation of n_1 and intrinsic birefringence than is possible by visual methods of determining the maximum or minimum of the Ambronn curve.

After the coefficients for the equation are determined, the easiest way to determine both n_1 and $(n_e - n_0)_i$ is to find the value of x at which the curve passes through a minimum ($x_{\min}$), which is where $n_1 = n_2$. This point is determined by setting the first derivative of Equation (14) equal to zero,

$$\frac{dy}{dx} = a_1 + 2a_2x + \cdots + na_nx^{(n-1)} = \sum_{i=1}^{n} [ia_i\, x^{(i-1)}] = 0 \tag{15}$$

and solving the resulting $(n - 1)$-order equation for $x_{\min}$. Only one of the values obtained should be within the experimental domain of x, and at this point

$$\sqrt{x} = \sqrt{(n_2)^2} = \sqrt{(n_1)^2} = n_1. \tag{16}$$

Placing this value of $x_{\min}$ back into Equation (14) gives the value of the intrinsic birefringence, since the form birefringence is zero where $n_1 = n_2$:

$$(n_e - n_o)_i = y_{\min} \times 10^{-3} = \left[\sum_{i=0}^{n} a_i(x_{\min})^i\right] \times 10^{-3}. \tag{17}$$

By reducing F, the Wiener form factor, to a generalized expression, it has been possible to avoid having to make any assumptions concerning the nature of the submicroscopic elements causing the form birefringence, up to this point in the derivation. By replacing the generalized F with one of the specific forms from Equation (8) or (9), or with any similar expression that might be derived for a different ideal system, it is possible to determine to what extent such expressions apply to the experimental system in question, by using them to calculate the volume fractions V_1 and V_2. The following equations assume that the experimental data is well fitted by a cubic equation; if it is necessary to use higher order equations to fit the experimental points, this is an indication that the specific forms of the Wiener equations do not apply, as shown earlier.

The simplest expression for F is at $x_{\min}$, where $n_1 = n_2$; at this point, from Equation (8),

$$F_{\text{rods}} = \frac{V_1V_2}{4n_1^3} \tag{18}$$

and from Equation (9),

$$F_{\text{plates}} = \frac{V_1V_2}{2n_1^3}. \tag{19}$$

Since F, for either structural system, will be a maximum when $V_1 = V_2 = 0.5$, the maximum possible theoretical value for F will be ($\frac{1}{16}\, n_1^3$) for rods, or ($\frac{1}{8}\, n_1^3$) for plates.

The numerical values for F used to solve these equations are determined for the fitted coefficients, since from Equations (12) and (13),

$$M = (a_3 \times 10^{-3}) \tag{20}$$

and

$$B = (a_2 \times 10^{-3}) + 2n_1^2M. \tag{21}$$

Substituting the above values of M and B into Equation (11), at $x_{\min}$,

$$F = 3(a_3 \times 10^{-3})n_1^2 + (a_2 \times 10^{-3}), \tag{22}$$

and from this, Equation (18), and the fact that $V_1 + V_2 = 1$, the volume fraction of the solid phase in a system of rods can be determined from

$$\frac{V_1\,(1 - V_1)}{4n_1^3} = 3(a_3 \times 10^{-3})\, n_1^2 + (a_2 \times 10^{-3}), \tag{23}$$

or

$$V_1^2 - V_1 + 12(a_3 \times 10^{-3})n_1^5 + 4(a_2 \times 10^{-3})n_1^3 = 0. \quad (24)$$

The quadratic solution of this equation gives two values (which are actually V_1 and V_2, since Equations [23] and [24] could have been written in terms of V_2 instead). The assignment of these two values to V_1 and V_2 must depend on the physical properties of the system, if they are known, since the theoretical equation does not distinguish between V_1 and V_2.

The same treatment, applied to Equations (19) and (22), gives an equation for the volume fractions for a system of plates:

$$V_1^2 - V_1 + 6(a_3 \times 10^{-3})n_1^5 + 2(a_2 \times 10^{-3})n_1^3 = 0. \quad (25)$$

The extent to which these calculated volume fractions are physically realistic for the experimental system provides a test of the assumptions on which the calculations are based; the rigorousness of such a test, however, is limited by the amount of information which can be determined independently of birefringence measurements. If no such information is available, which is the case for the sperm cells in this paper, then the assumption of ideal rods, or plates, can be ruled invalid only if it produces volume fractions which are completely unrealistic (negative, imaginary, or greater than one). A calculation of the volume fractions from some other method (such as electron microscopy) provides a much more critical test of the assumptions, since a quantitative comparison is then possible.

REFERENCES

ALTMAN, P. L., and D. S. DITTMER, editors. 1962. Growth, Including Reproduction and Morphological Development. Federation of American Societies for Experimental Biology, Washington, D.C. 163.

AMBRONN, H. 1916. *Kolloid Z.* **18**:90.

AMBRONN, H., and A. FREY. 1926. Das Polarisationsmikroskop. Akademische Verlagsgesellschaft, Leipzig.

BENEDICT, R. C. 1964. Ph.D. Thesis. University of Pennsylvania, Philadelphia.

CASSIM, J. Y., P. S. TOBIAS, and E. W. TAYLOR. 1968. *Biochim. Biophys. Acta.* **168**:463.

DALLAM, R. D., and L. E. THOMAS. 1953. *Biochim. Biophys. Acta.* **11**:79.

FREY, A. 1926. *Jahrb. Wiss. Bot.* **65**:195.

FREY-WYSSLING, A. 1948. Submicroscopic Morphology of Protoplasm and Its Derivatives. Elsevier Publishing Co., Amsterdam. 58.

FREY-WYSSLING, A. 1964. *In* Formation of Wood in Forest Trees. Academic Press Inc., New York.

FREY-WYSSLING, A., and K. MÜHLETHALER. 1965. Ultrastructural Plant Cytology. Elsevier Publishing Co., Amsterdam.

FREY-WYSSLING, A., and E. STEINMANN. 1948. *Biochim. Biophys. Acta.* **2**:254.

HARTSHORNE, N. H., and A. STUART. 1970. Crystals and the Polarising Microscope. Edward Arnold Publishers Ltd., London. 4th edition.

INOUÉ, S., and H. SATO. 1966. *In* Molecular Architecture in Cell Physiology. T. Hayashi and A. G. Szent-Gyorgyi, editors. Prentice-Hall, Inc., Englewood Cliffs, N. J. 209.

KOEHLER, J. K. 1966. *J. Ultrastruct. Res.* **16**:359.

KOEHLER, J. K. 1968. *Advan. Biol. Med. Phys.* **12**:1.

KOEHLER, J. K. 1970. *J. Ultrastruct. Res.* **33**:598.

LAUFFER, M. A. 1938. *J. Phys. Chem.* **42**:935.

LUNG, B. 1968. *J. Ultrastruct. Res.* **22**:485.

PETERLIN, A., and H. A. STUART. 1939. *Z. Phys.* **112**:1.

SATO, H., and S. INOUÉ. 1964. *Biol. Bull. (Woods Hole).* **127**:357.

SATO, H., S. INOUÉ, and G. W. ELLIS. 1971. Abstracts of Papers Presented at the 11th Annual Meeting of the American Society for Cell Biology. 261.

SCHMIDT, W. J. 1928. *Zool. Jahrb. Abt. Allg. Zool. Physiol. Tiere.* **45**:177.

WALKER, H. M., and J. LEV. 1958. Elementary Statistical Methods. Holt, Rinehart, and Winston, Inc., New York.

WIENER, O. 1912. *Abh. Math. Phys. Kl. Saechs. Akad. Wiss.* **32**:507.